Available online at www.sciencedirect.com
ScienceDirect
Journal of Power Sources 174 (2007) 380–386
JOURNAL OF POWER SOURCES
www.elsevier.com/locate/jpowsour

Investigation of positive electrodes after cycle testing of high-power Li-ion battery cells I. An approach to the power fading mechanism using XANES

Hironori Kobayashi *, Masahiro Shikano, Shinji Koike, Hikari Sakaebe, Kuniaki Tatsumi

Research Institute for Ubiquitous Energy Devices, National Institute of Advanced Industrial Science and Technology (AIST), Ikeda, Osaka 563-8577, Japan

Available online 28 June 2007

Abstract

Cylindrical lithium-ion (Li-ion) cells with a nickel-cobalt oxide ($LiNi_{0.73}Co_{0.17}Al_{0.10}O_2$) positive electrode and a non-graphitizable carbon (hard carbon) negative electrode were degraded using cycle tests. The degraded cells were disassembled and examined; most attention was paid to the positive electrodes in order to clarify the origin of the power fade of the cells. X-ray absorption near-edge structure (XANES) analysis demonstrated that the crystal structure of the electrode at the surface changed from rhombohedral to cubic symmetry. Furthermore, a film of lithium carbonate (Li_2CO_3) covered the surface of the positive electrode after the cycle tests. Using a combination of X-ray photoelectron spectroscopy (XPS), infrared spectroscopy (IR), and glow discharge optical emission spectrometry (GD-OES) measurements, a schematic model of the changes occurring in the surface structure of the positive electrode during the cycle tests was constructed. The appearance of both an electrochemically inactive cubic phase and lithium carbonate films at the surface of the positive electrode are important factors giving rise to power fade of the positive electrode.

Keywords: Layered oxides; Lithium nickel-based oxide; Cathode material for lithium secondary batteries; Synchrotron radiation; XAFS measurements

1. Introduction

Several of the requirements of rechargeable batteries for hybrid electric vehicles (HEVs) and fuel cell vehicles (FCVs) are quite different to those of portable electronic devices such as cellular phones and laptop computers. In particular, high specific power and long calendar life are very important requirements of HEV and FCV applications. Recently, much effort has been applied to understanding the mechanisms that limit the calendar life of high-power lithium-ion (Li-ion) cells that have been developed for use in HEVs as part of the Advanced Technology Development (ATD) program in the United States [1–6]. In this program, the capacities and pulse power capabilities of 1 Ah capacity, 18650-type cells have been measured under various experimental conditions to determine the components that limit cell performance. The aim is to identify and replace these components with alternative materials to enable the development of safer, longer-life Li-ion batteries. In Japan, the national R&D project entitled "Development of Lithium Battery Technology for Use by Fuel Cell Vehicles" has been promoted by the New Energy and Industrial Technology Development Organization (NEDO), which has set targets for specific power and calendar life of 1800 W kg^{-1} and 15 years, respectively. Since both targets are beyond the requirements of most portable electronic device applications, it is necessary to develop not only technologies for achieving these targets but also methods of evaluation. Thus, in the NEDO R&D project on lithium batteries there is a line of research dedicated to establishing evaluation methods and accelerated life tests that are suitable for each type of cell chemistry. In order to establish accelerated calendar life tests, a collaboration framework has been built. As part of this framework, three battery manufacturers (Matsushita Battery Industrial, GS-Yuasa Corporation, and Hitachi Vehicle Energy) provided the Central Research Institute of Electric Power Industry (CRIEPI) with cells, where various evaluation tests and life tests were carried out [7,8]. These cells were then transferred to the National Institute of Advanced Industrial Science and Technology (AIST) in order to analyze the degradation of the battery materials (active materials, electrolytes, current collectors, etc.) accompanying the power fade and decrease in capacity [9–11]. Several mechanisms for the degradation of lithium batteries have been proposed [7,8,12]. In order to achieve the target of at least

* Corresponding author. Tel.: +81 727 51 7932; fax: +81 727 51 9609.
E-mail address: hironori-kobayashi@aist.go.jp (H. Kobayashi).

0378-7753/$ – see front matter © 2007 Elsevier B.V. All rights reserved.
doi:10.1016/j.jpowsour.2007.06.134

15 years, the development of a method of projecting calendar life is urgently needed. The goal of our project is to develop an understanding of the effect of accelerated calendar life testing on the performance of Li-ion battery cells by constructing a model of the degradation process. Therefore, it is very important to understand the origin of the degradation of electrochemical performance.

In the ATD program, 18650-type high-power Li-ion cells (Gen 1) have been designed and fabricated in order to investigate the factors limiting the calendar life of lithium batteries. These cells consisted of a $LiNi_{0.8}Co_{0.2}O_2$-based positive electrode, a negative electrode comprised of a blend of MCMB-6 and SFG-6 carbon, and a $LiPF_6$ in EC:DEC (1:1) electrolyte. After accelerated calendar life and cycle life testing at elevated temperatures, the cells experienced a significant rise in impedance and loss of power. The power fade rate was dependent on both the state of charge and the temperature of testing. Micro-reference electrode and ac-impedance studies on symmetrical cells have confirmed that the interfacial resistance at the positive electrode is the main reason for the impedance rise in high-power cells [2]. Structural and electrical investigations have been conducted on lithium nickel oxide-based particles used in positive electrodes. Using oxygen K-edge X-ray absorption spectroscopy (XAS), high resolution transmission electron microscopy (HRTEM), nanoprobe diffraction (ND), and electron energy loss spectroscopy (EELS), a modified layer of less than 5 nm thickness was detected on the surface of the oxide particles after the cycle tests [5]. This modified layer results from the loss of cation ordering between Ni and Li in the layered $R\bar{3}m$ structure of the electrode material, caused by oxygen deficiency and lower Ni- and Co-oxidation states near the surface after cycling. X-ray photoelectron spectroscopy (XPS) revealed that a mixture of organic species such as polycarbonates, LiF, Li_xPF_y-type and $Li_xPF_yO_z$-type compounds formed a surface film on the positive electrodes regardless of the temperature or duration of the test or the state-of-charge [6]. Growth of the modified layer and the surface film may contribute to the rise in impedance of the positive electrode, in particular giving rise to a charge-transfer resistance at the electrode/electrolyte interface.

Toyota Central R&D Labs Inc. have investigated the morphological changes of positive electrode particles and the local structure of the $LiNi_{0.8}Co_{0.2}O_2$-based electrode material in order to examine the mechanism of the increase in resistance [13]. An increase in the resistance of cells comprised of a $LiNi_{0.8}Co_{0.2}O_2$-based material and artificial graphite was observed in cycling tests at 60 °C; a "cell reconstruction" method demonstrated that it could be mainly attributed to the positive electrode. The focused ion beam (FIB) technique revealed the formation of space and cracks at grain boundaries inside the particles after cycling. Furthermore, in-situ X-ray absorption fine structure spectroscopic (XAFS) measurements showed that a change in the local structure around the Co-atom takes place during the charge–discharge process at 60 °C. It was thus concluded that both morphological and local structural changes of the positive electrode material give rise to the increase in resistance.

Although the deterioration in the performance of currently available lithium batteries is thought to result from problems with the positive electrodes, the mechanism of deterioration of the electrodes is still poorly understood. Detailed information on the changes taking place in both the cathode and anode on cycling is essential in order to determine the origin of the degradation of performance. We have previously reported that combined soft and hard synchrotron X-ray absorption near-edge structure (XANES) analyses, which provide complementary information, is a powerful method for investigating changes in surface structure [14,15]. In this study, $LiNi_{0.73}Co_{0.17}Al_{0.10}O_2$ positive electrodes from cells that had undergone power fading through cycling tests were examined by XANES analysis to obtain information on their surfaces. The relationship between power fade and the surface state of the positive electrode will be discussed.

2. Experimental

We used cylindrical battery cells of capacity 400 mAh for this study, which were designed to have a rate capability of more than 10 C. The cells were constructed from pressed double-side coated electrodes using a high-power design; the positive electrode was comprised of $LiNi_{0.73}Co_{0.17}Al_{0.10}O_2$, acetylene black (AB), and poly(vinyldene fluoride) (PVdF) binder, and the negative electrode consisted of non-graphitizable carbon (hard carbon) and PVdF binder. The electrolyte was 1 mol dm^{-3} $LiPF_6$ in propylene carbonate (PC)/diethylcarbonate (DMC) (volume ratio 3:2).

The cells were degraded by carrying out cycle tests, determined by CRIEPI, in which they were charged to 50% state-of-charge (SOC) and tested with a 3% depth-of-discharge (DOD) at various temperatures under the current profile shown in Fig. 1. Each cell was characterized using the standard battery test procedure given in the partnership for a new generation of vehicles (PNGV) Battery Test Manual [16]. The changes in cell capacity and dc resistance were checked every few cycles. The dc resistance of the cell was estimated, as shown in Fig. 2, by plotting the cell voltage at 10 s after the start of discharge against the discharge pulse current; the dc resistance was calculated from the slope of $-\Delta V/\Delta I$. A linear relationship was found between the voltage of the cell at 50% SOC and the discharge pulse current. This demonstrates that our cells have a rate capa-

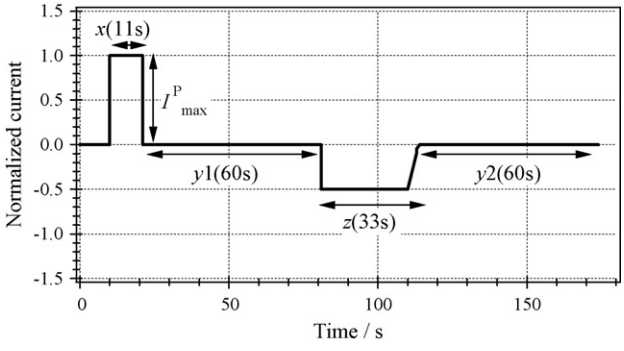

Fig. 1. Current profile of cycle tests carried out in present experiment.

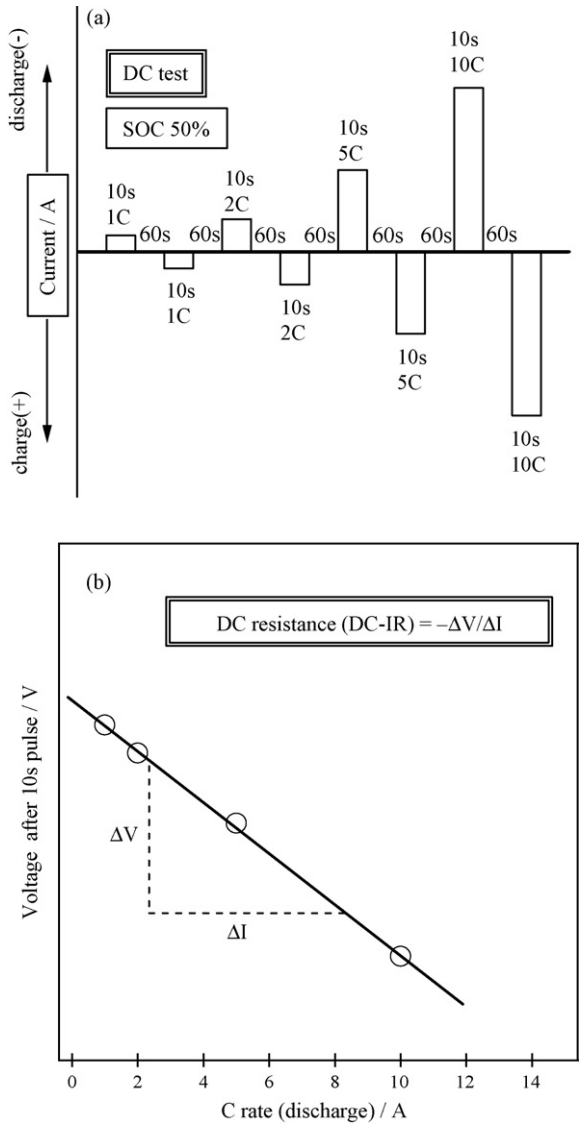

Fig. 2. Pulse current profile used for calculation of dc resistance (a) and C-rate dependence of the cell voltage (b).

bility of more than 10 C. After completion of the degradation test, the SOC of the cell was adjusted to 0% or 100% immediately before disassembling it, since the chemical and physical properties of the active materials are influenced by the SOC. After disassembly of the SOC-adjusted cell, the surface of the positive electrode was examined by XANES in order to study the surface film or phase transitions in particles of the active material.

The M $L_{II,III}$-edge and O K-edge XANES spectra of the samples were measured on the BL1A, BL8B1, and BL4B beamlines of the UVSOR Facility at the Institute for Molecular Science (Proposal Nos. 16-557 and 18-229). Data were obtained in the total electron yield (TEY) and fluorescence yield (FY) modes. The M K-edge XAFS spectra of the samples were measured on the BL7C beamline of the Photon Factory at the National Laboratory for High Energy Physics (KEK-PF, Proposal No. 2001G123). The measurements were performed in transmission mode and the incident X-rays were monochromatized with a Si(1 1 1) crystal. The extended X-ray absorption fine structure (EXAFS) data were analyzed using Rigaku REX2000 software. The backgrounds were subtracted using an extrapolated Victoreen-plus-constant type function and the EXAFS oscillations $\chi(k)$ were extracted using cubic spline baseline functions. Fourier transforms were performed on the normalized $\chi(k)$ with k^3 weighting of a Hanning window in the region $k = 2.5$–15.0 for the Mn K-edge and $k = 2.5$–12.0 for the Co K-edge. The change in local structure around the M cations was determined by curve fitting, which was carried out using a one-shell model in the filtered range $R = 1.0$–2.0 Å for M–O. We neglected the scattering from the Li atoms in our analysis since the photoelectron backscattering amplitude from Li is very weak. The coordination number of M was fixed at 6.

3. Results and discussion

3.1. Performance of the test cells

Fig. 3 shows the cycle dependence of the cell capacity and dc resistance; the values at the end of each test are summarized in Table 1. The test cell data were collected by Dr. Kihira at CRIEPI [7,8]. The relative capacity decreased from 0.960 to 0.808 and the relative dc resistance increased from 1.08 to 1.74 on increasing the test temperature from 20 °C to 80 °C. Above 80 °C, an abrupt decrease in capacity and an increase in dc resistance were observed.

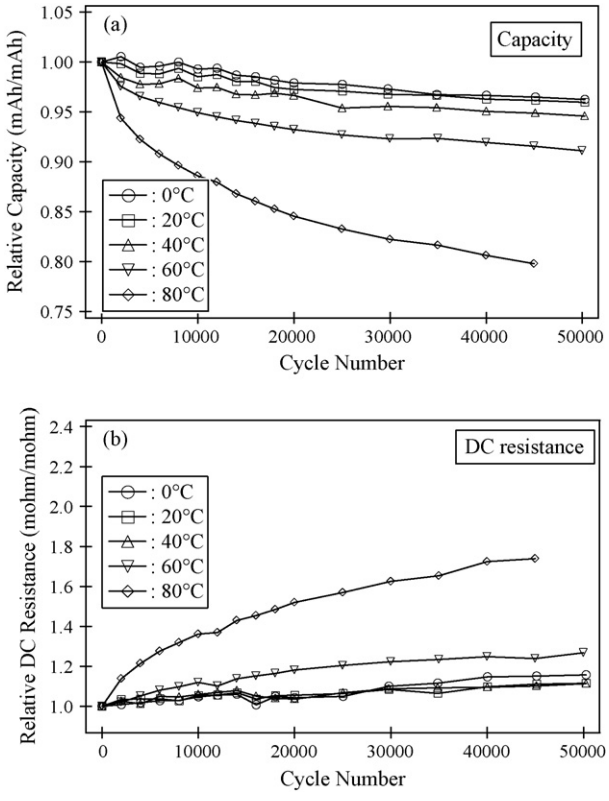

Fig. 3. Cycle dependence of retention of capacity and dc resistance. These data were collected by Dr. Kihira at CRIEPI [7,8].

Table 1
Summary of cycle tests

No.	Temperature (°C)	I^{P}_{max} (C)	DOD (%)	Cycles	Relative capacity	Relative dc resistance
1	0	10	3	50,000	0.962	1.16
2	20	10	3	50,000	0.960	1.11
3	40	10	3	50,000	0.946	1.11
4	60	10	3	50,000	0.911	1.27
5	80	10	3	45,000	0.798	1.74

3.2. Context from previous results

In our previous work [9,10], XRD and ND measurements of the degraded positive electrode showed no peak broadening and no additional peaks from impurity phases, indicating that the bulk structure of $Li_xNi_{0.73}Co_{0.17}Al_{0.10}O_2$ was essentially unchanged even after 50,000 cycles. The Li content at 0% SOC abruptly decreased at 60 °C, corresponding to a large decrease in capacity retention. This result implies that on discharge, not all of the Li-ions returned to the positive electrode, leading to a decrease in capacity. For the hard carbon negative electrode, the Li content was estimated using ^{7}Li NMR measurements. In general, there is a positive correlation between the NMR shift of ^{7}Li and the Li content in hard carbon [17]. An increase in the NMR shift of Li with increasing capacity fade at 100% SOC showed that more Li-ions are inserted into the hard carbon electrode after the degradation tests. Therefore, this imbalance in the Li contents of the positive and negative electrodes is one of the most important causes of capacity fade. It has also been suggested that the increase in resistance of Li-ion cells containing a $LiNi_{0.80}Co_{0.15}Al_{0.05}O_2$ positive electrode and a carbon negative electrode can mainly be attributed to an increase in resistance of the positive electrode [2]. However, our results indicated that the bulk structure of the positive electrode was essentially unchanged, even after degradation testing [7]. Therefore, we examined the surface structure of the $Li_xNi_{0.73}Co_{0.17}Al_{0.10}O_2$ positive electrode by XANES measurements.

3.3. XANES and EXAFS analyses for Ni and Co

In order to obtain information on the surface of the $Li_xNi_{0.73}Co_{0.17}Al_{0.10}O_2$ positive electrode, we collected Ni and Co L-edge XANES spectra in TEY mode using soft X-rays. Fig. 4 shows the Ni and Co $L_{III,II}$-edge XANES spectra before and after performing the cycle tests. The spectra of NiO and $LiCoO_2$ are also shown, serving as reference compounds for Ni^{2+} and Co^{3+}, respectively. The Ni L-edge spectrum of the positive electrode before cycle testing showed a significant shift of the peak position to higher energy on increasing the SOC. In contrast, the peak position in the Co L-edge spectrum of the positive electrode before cycle testing was the same at both 0% and 100% SOC. Therefore, the valence states of Ni and Co were Ni^{3-4+} and Co^{3+}. Both Ni and Co L-edges XANES spectra collected from 100% SOC samples showed shifts of the L_{III} and L_{II} peaks to higher energy above 40 °C, indicating that a slight increase in the valence states of Ni and Co occurs at the surface after cycling tests performed at higher temperatures.

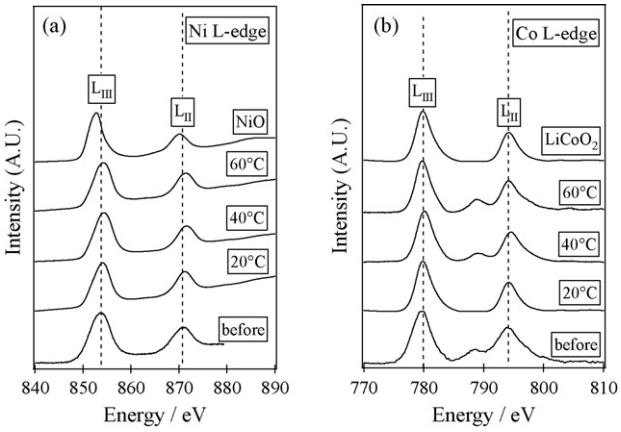

Fig. 4. Ni (a) and Co (b) $L_{III,II}$-edge XANES spectra of the $Li_xNi_{0.73}Co_{0.17}Al_{0.10}O_2$ positive electrode before and after cycle tests.

In order to obtain information on the changes occurring in the bulk structure of the $Li_xNi_{0.73}Co_{0.17}Al_{0.10}O_2$ positive electrode, M K-edge XAFS spectra were measured using hard X-rays. Fig. 5 shows the Ni and Co K-edge XANES spectra before and after the cycle tests. The spectra of $LiNiO_2$ and $LiCoO_2$ are also shown, serving as reference compounds for Ni^{3+} and Co^{3+}, respectively. Both the Ni and Co K-edge XANES spectra display a continuous shift to higher photon energy with increas-

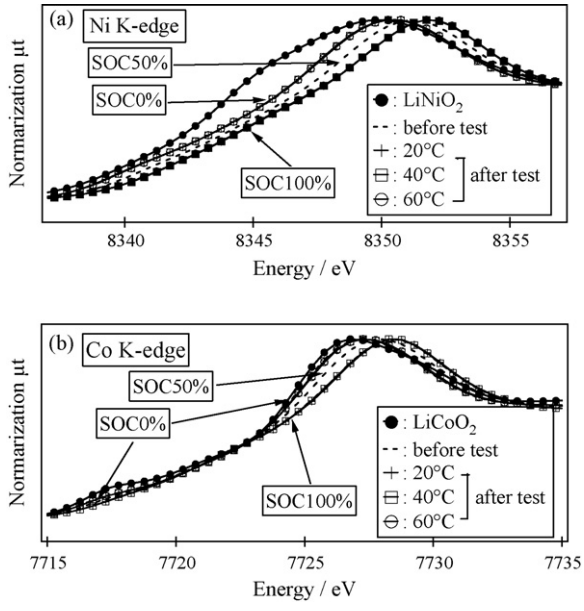

Fig. 5. Ni (a) and Co (b) K-edge XANES spectra of the $Li_xNi_{0.73}Co_{0.17}Al_{0.10}O_2$ positive electrode before and after cycle tests.

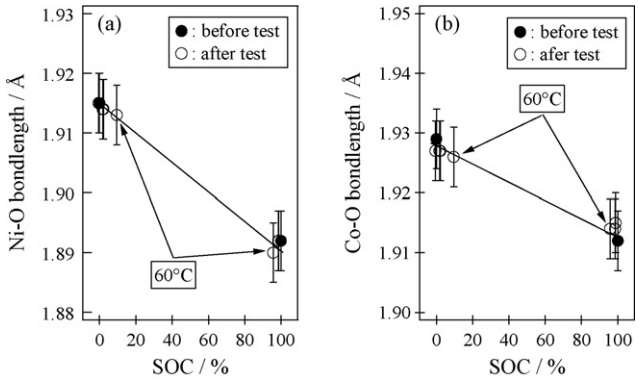

Fig. 6. SOC dependence of the M–O bondlength in the $Li_xNi_{0.73}Co_{0.17}Al_{0.10}O_2$ positive electrode before and after cycle tests.

ing SOC, indicating a valence state changing between Ni^{3+}/Ni^{4+} and Co^{3+}/Co^{4+}. In contrast, there was little shift in energy for spectra measured before and after the cycle tests for either 0% or 100% SOC, indicating that no change in valence state occurs during the cycle tests from the viewpoint of bulk structure. These results were supported by EXAFS measurements. Fig. 6 shows the SOC dependence of the M–O bond length in the $Li_xNi_{0.73}Co_{0.17}Al_{0.10}O_2$ positive electrode before and after the cycle tests. The oxidation of Ni and Co with increasing SOC is clearly illustrated; the Ni–O and Co–O bond lengths decrease from 1.92 Å (0% SOC) to 1.89 Å (100% SOC) and from 1.93 Å (0% SOC) to 1.91 Å (100% SOC), respectively. The Ni–O and Co–O bond lengths showed essentially no change before and after the cycle tests, even at 60 °C. Thus, XAFS analysis has demonstrated that the valence states of Ni and Co at the surface of the $Li_xNi_{0.73}Co_{0.17}Al_{0.10}O_2$ positive electrode are slightly different to those of the bulk at 60 °C.

3.4. XANES analysis of oxygen

In order to obtain more information on the surface and bulk of the $Li_xNi_{0.73}Co_{0.17}Al_{0.10}O_2$ positive electrode, we measured O K-edge XANES spectra in TEY and FY modes, respectively, using soft X-rays. Fig. 7 shows the O K-edge XANES spectra of 100% SOC samples. In Fig. 7(a), the spectra of NiO and Li_2CO_3 are also shown as reference compounds. In TEY mode, O K-edge XANES spectra provide information on the surface structure. The spectrum measured before cycle testing contained peak A at approximately 529 eV, corresponding to oxygen originating from the layered structure, and peaks B and C at approximately 532 eV and 534 eV. After the cycle tests, the intensity of peak A clearly decreased at 60 °C, while the intensities of peaks B and C showed no significant changes. The position of peak B was close to that of the NiO reference sample spectrum, indicating the existence of a cubic phase on the surface, and the position of peak C was close to that of Li_2CO_3, or to conductive materials such as AB (data not shown). When measured in FY mode, O K-edge XANES spectra provide information on the bulk structure. Here, essentially the same spectra were observed before and after the cycle tests for all the samples. The strong peak A at 529 eV originating from the layered structure of the positive electrode

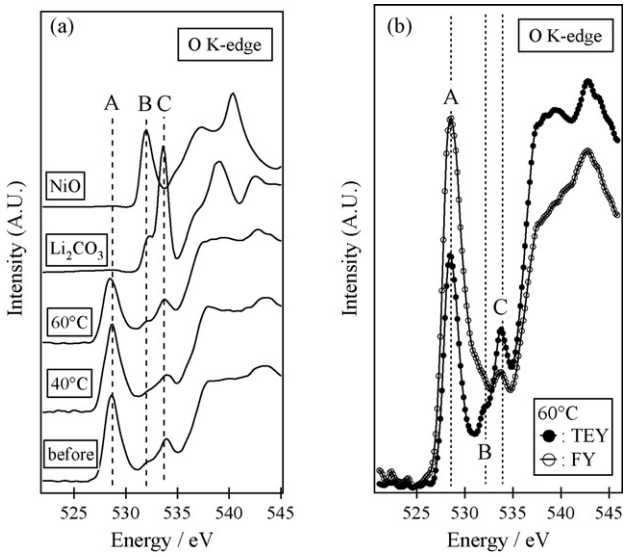

Fig. 7. O K-edge XANES spectra of the $Li_xNi_{0.73}Co_{0.17}Al_{0.10}O_2$ positive electrode, measured in TEY mode (a) and in both TEY and FY modes (b), before and after cycle tests.

was observed in FY mode, as shown in Fig. 7(b). However, peak B was absent and peak C was much lower in intensity. These results indicate that the surface structure is different to that of the bulk in this system. Furthermore, it is clear that part of the layered structure at the surface of the $Li_xNi_{0.73}Co_{0.17}Al_{0.10}O_2$ positive electrode was transformed to a cubic structure at 60 °C, although the layered structure was retained in the bulk. The surface of the active materials was covered with a film of Li_2CO_3.

3.5. Discussion

In the present study, XANES analysis has demonstrated that the surface region of the positive electrode underwent a transition from the rhombohedral phase to a lithium deficient cubic phase after cycle testing. Furthermore, the electrode was covered by a surface film of Li_2CO_3 after the cycle tests. Therefore, the presence of the cubic phase, most likely formed by decomposition of the layered structure due to a deficiency of lithium on the surface of the cathode, may be linked to the power fading of batteries.

Other members of our groups have studied the same system using XPS [18], attenuated total reflectance Fourier spectroscopy (ATR FT-IR) [19], and glow discharge optical emission spectrometry (GD-OES) [20]. Here we briefly review the main results and point to the corresponding references for more details. Shikano et al. used XPS to show that Li_2CO_3, hydrocarbons, $ROCO_2Li$, polycarbonate-type compounds, and LiF were all present on the cathode surface, and that the quantity of carbonates increased after cycle tests had been performed [18]. Signs of decomposition of the electrolyte were also observed at temperatures above 60 °C. Furthermore, there was shown to be an Li-deficient cubic phase near the surface of the positive electrodes, which increases with degradation. The decrease in capacity and the power fade that take place on cycling could thus be correlated with the quantity of impurity species on the

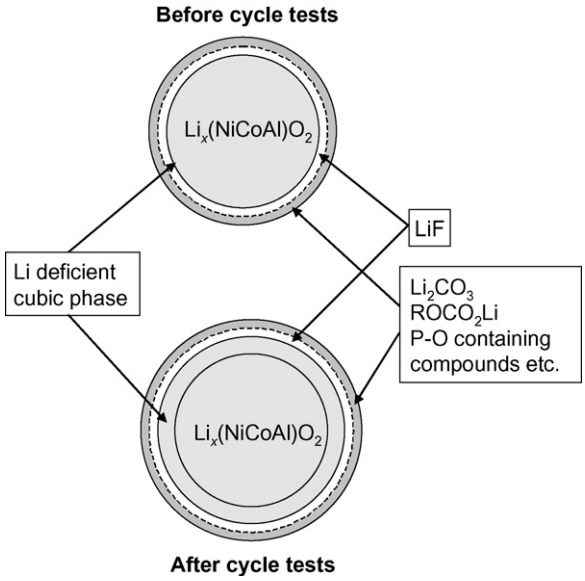

Fig. 8. Schematic representation of the surface structure of the $Li_xNi_{0.73}Co_{0.17}Al_{0.10}O_2$ positive electrode before and after cycle tests.

surface and with the thickness of the Li-deficient cubic phase near the surface. Rahman and co-workers used the ATR FT-IR technique to detect propylene carbonate (PC), Li_2CO_3, and P–O containing compounds formed by decomposition reactions of PC and $LiPF_6$ in the electrolyte [19]. Although the power fading was greater when the cycle tests were carried out at higher temperature, no strong correlation of the power fading with the quantity of impurity materials on the surface was observed. Saito and co-workers used the GD-OES technique to observe an almost homogeneous concentration profile of lithium despite variations in sample depth; this was the case even for a sample tested at 80 °C [20]. This suggests that particles of active material deep inside the electrode layer are involved in the electrochemical reaction as well as particles in the surface area. In addition, the observation of particle morphology by SEM after the cycle tests showed that, although small fractures were visible at grain boundaries inside the particles, no actual cracks in the $Li_xNi_{0.73}Co_{0.17}Al_{0.10}O_2$ positive electrode were evident.

Combining the results of the XANES, XPS, IR, and GD-OES measurements, a schematic model to describe the changes taking place in the surface structure of the positive electrode during cycle testing was constructed, as shown in Fig. 8. The appearance of the electrochemically inactive cubic phase and surface films (consisting of Li_2CO_3, hydrocarbons, $ROCO_2Li$, polycarbonate-type compounds, P–O containing compounds, and LiF) at the $Li_xNi_{0.73}Co_{0.17}Al_{0.1}O_2$ positive electrode are important factors giving rise to power fade.

4. Conclusion

The Ni and Co K- and L-edge XAFS analysis has demonstrated that the valence state of Ni and Co at the surface of the $Li_xNi_{0.73}Co_{0.17}Al_{0.10}O_2$ positive electrode was the same as that of the bulk even after cycle testing, and increased only slightly when the tests were carried out at elevated temperatures. The O K-edge XANES results indicated that the surface structure becomes different to that of the bulk after cycle tests. The measurements indicate that a cubic phase is formed from the layered structure, probably due to a deficiency of lithium cations. Furthermore, a film of Li_2CO_3 is formed on the surface of the positive electrode. We conclude that XAFS analysis using a combination of hard and soft X-ray data is a powerful method for investigating the surface structure of cathode materials. A schematic model of the changes occurring in the surface structure of the positive electrode during cycle testing was constructed using the results of XANES, XPS, FT-IR, and GD-OES measurements. It is clear that the appearance of the electrochemically inactive cubic phase and the formation of surface films at the positive electrode are factors affecting the power fade in these Li-ion batteries.

Acknowledgements

This work was carried out in the "Development of Lithium Battery Technology for Use by Fuel Cell Vehicles" program of the New Energy and Industrial Technology Development Organization (NEDO) with the financial support of the Ministry of Economy, Trade and Industry (METI) and NEDO. The authors would like to thank Mr. Y. Ozaki of Matsushita Battery Industrial for providing the battery cells used in this research. The authors would also like to thank Dr. Y. Kihira of CRIEPI for providing the cells degraded by cycle testing.

References

[1] K. Amine, J. Liu, ITE Lett. 1 (2000) 59–63.
[2] K. Amine, C.H. Chen, J. Liu, M. Hammond, A. Jansen, D. Dees, I. Bloom, D. Vissers, G. Henriksen, J. Power Sources 97–98 (2001) 684–687.
[3] I. Bloom, B.W. Cole, J.J. Sohn, S.A. Jones, E.G. Polzin, V.S. Battaglia, G.L. Henriksen, C. Motloch, R. Richardson, T. Unkelhaeuser, D. Ingersoll, H.L. Case, J. Power Sources 101 (2001) 238–247.
[4] R.B. Wrighta, C.G. Motlocha, J.R. Belta, J.P. Christophersena, C.D. Hoa, R.A. Richardsona, I. Bloomb, S.A. Jonesb, V.S. Battagliab, G.L. Henriksenb, T. Unkelhaeuserc, D. Ingersollc, H.L. Casec, S.A. Rogersd, R.A. Sutula, J. Power Sources 110 (2002) 445–470.
[5] A.M. Andersson, D.P. Abraham, R. Haasch, S. MacLaren, J. Liu, K. Amine, J. Electrochem. Soc. 149 (2002) A1358–A1369.
[6] D.P. Abraham, R.D. Twesten, M. Balasubramanian, J. Kropf, D. Fischer, J. McBreen, I. Petrov, K. Amine, J. Electrochem. Soc. 150 (2003) A1450–A1456.
[7] N. Kihira, Y. Mita, K. Takei, Y. Kobayashi, H. Miyashiro, K. Kumai, N. Terada, T. Iwahori, Abstracts of the 206th ECS Meeting, 2004,p. 385.
[8] N. Kihira, N. Terada, Proceedings of the 22nd International Battery, Hybrid and Fuel Cell Electric Vehicle Symposium and Exposition in Japan,2006.
[9] H. Kobayashi, S. Koike, M. Shikano, H. Sakaebe, K. Tatsumi, Abstracts of the 45th Battery Symposium in Japan, 2004, pp. 528–529.
[10] H. Kobayashi, S. Koike, M. Shikano, H. Sakaebe, K. Tatsumi, Abstracts of the 46th Battery Symposium in Japan, 2005, pp. 556–557.
[11] K. Tatsumi, H. Kobayashi, M. Shikano, S. Koike, H. Sakaebe, Y. Saito, Md.K. Rahman, Proceedings of the 22nd International Battery, Hybrid and Fuel Cell Electric Vehicle Symposium and Exposition in Japan, 2006.
[12] Y. Saito, J. Power Sources 146 (2005) 770–774.
[13] Y. Itou, Y. Ukyo, J. Power Sources 146 (2005) 39–44.
[14] H. Kobayashi, Y. Arachi, S. Emura, H. Kageyama, K. Tatsumi, T. Kamiyama, J. Power Sources 146 (2005) 640–644.

[15] H. Kobayashi, Y. Arachi, S. Emura, K. Hannda, K. Tatsumi, AIP Conference Proceedings of X-ray Absorption Fine Structure—XAFS-13, vol. 882, 2007, pp. 478–480.
[16] PNGV Battery Test Manual, Rev. 3, DOE/ID-10597, 2001.
[17] K. Tatsumi, T. Kawamura, S. Higuchi, T. Hosotubo, H. Nakajima, Y. Sawada, J. Power Sources 68 (1997) 263–266.
[18] M. Shikano, H. Kobayashi, S. Koike, H. Sakaebe, E. Ikenaga, K. Kobayashi, K. Tatsumi, J. Power Sources 174 (2007) 795.
[19] Y. Saito, Md.K. Rahman, J. Power Sources 174 (2007) 877.
[20] Md.K. Rahman, Y. Saito, J. Power Sources 174 (2007) 889.